// Hamburger Beiträge
zur Angewandten Mathematik

The Quadrant Hausdorff Distance: A Metric of Image Quantization

Ari Gross and Longin Jan Latecki

Reihe A
Preprint 142
June 1999

Hamburger Beiträge zur Angewandten Mathematik

Reihe A	Preprints
Reihe B	Berichte
Reihe C	Mathematische Modelle und Simulation
Reihe D	Elektrische Netzwerke und Bauelemente
Reihe E	Scientific Computing
Reihe F	Computational Fluid Dynamics and Data Analysis

The Quadrant Hausdorff Distance: A Metric of Image Quantization

Ari Gross*   Longin Jan Latecki†

June 18, 1999

Abstract

In this paper we introduce a new similarity metric for planar point sets called the *quadrant Hausdorff distance*. This new metric is a modification of the Hausdorff distance that is consistent with the digitization process:

Any two digital objects differ by at most quadrant Hausdorff distance one if and only if there is a planar object that digitizes to both of them under an idealized model of the digitization process.

The implication "⇒" does not hold for Hausdorff distance, i.e., if two digital objects differ by at most Hausdorff distance one, there does not necessarily exist a planar object that digitizes to both of them. However, in many applications on digital sets such as character recognition, bitmaps are often grouped into equivalence classes and considered to be digitizations of the same continuous prototype character based on Hausdorff distance one.

The consistency of the quadrant Hausdorff distance with the digitization process gives us a theoretical foundation to treat digital sets that differ by at most quadrant Hausdorff distance one as digital images of the same continuous object, since such an object exists. This implies that using the quadrant Hausdorff distance instead of the Hausdorff distance will lead to a significant reduction in the number of mismatches.

Although the quadrant Hausdorff distance is more restrictive than the Hausdorff distance, it does not eliminate any matches in an idealized scanner digitization, since any two digital images of the same planar object can differ by no more than quadrant Hausdorff distance one. This fact is also empirically justified by numerous experimental results in character recognition.

*Dept. of Computer Science, Queens College, CUNY, Flushing, New York 11367, USA; ari@vision.cs.qc.edu

†Dept. of Applied Mathematics, University of Hamburg, Bundesstr. 55, 20416 Hamburg, Germany; latecki@math.uni-hamburg.de

1 Introduction

The discrete definition of the Hausdorff distance of sets is used for comparison of digital sets in computer vision (Huttenlocher et al. [2]). Since the Hausdorff distance is not reflection, rotation, and scale invariant, it is mostly used in applications, where the compared objects do not differ by these transformations, which is, for example, the case in character recognition and compression of document images.

In this paper we examine properties of the Hausdorff distance with respect to a mathematical model of the digitization process of scanners, in which there is no noise or blurring in the digitization process. Thus, the "digitization error" is only due to the translation of the object with respect to the square grid.

We propose a modification of the Hausdorff distance called the quadrant Hausdorff distance, (hereafter QH distance). The fact that the QH distance H_Q is consistent with the digitization process is described by the following theorem (proved in Section 3):

It holds $H_Q(A, B) \leq 1$ for any two digital sets A and B iff there exist a continuous set X and a translation vector $v \in \mathbb{R}^2$ such that $Dig(X) = A$ and $Dig(X + v) = B$, where $Dig : \mathbb{R}^2 \to \mathbb{Z}^2$ is the digitization mapping.

This theorem motivates consideration of A and B as digital images of the same continuous set, whose positions with respect to the grid differ by translations.

We show with a simple example in Section 3 that this theorem does not hold for the Hausdorff distance, i.e., the implication "$\Rightarrow$" does not hold.

In applications, however, it is often the case that digital sets are incorrectly treated as images of the same continuous set if their Hausdorff distance is smaller than or equal to one. In these applications, the usage of the QH distance instead can lead to significant improvements, e.g., to a reduction in recognition errors in the character recognition process. This theoretical implication has been confirmed by a large number of experimental results.

Although the quadrant Hausdorff distance is more restrictive than the Hausdorff distance, it does not eliminate any matches in an idealized scanner digitization due to the "$\Leftarrow$" implication, i.e., any two digital images of the same planar object can differ by no more than quadrant Hausdorff distance one. We present experimental results to illustrate this claim in Section 5.

We show that QH distance H_Q is a metric for the L_∞ Distance in Section 4.

2 Definitions

We assume that all continuous sets are closed and bounded subsets of the plane. We will consider three different metrics on the plane $\mathbb{R}^2$: Euclidean distance, L_∞ distance (i.e., *max* distance), and L_1 distance (i.e., city block distance). The L_∞ distance restricted to $\mathbb{Z}^2 \subseteq \mathbb{R}^2$ is called 8-distance and the L_1 distance is called 4-distance.

For $n = 4$ or 8, the n-**neighborhood** of a point $P = (x, y)$ in $\mathbb{Z}^2$ is the set $\mathcal{N}_n(P)$ consisting of P and its n-neighbors. $\mathcal{N}_n^*(P)$ is the set of all neighbors of P without P itself. Note that $\mathcal{N}_n^*(P) = \mathcal{N}_n(P) \setminus \{P\}$. The points in $\mathcal{N}_8^*(P)$ are numbered 0 to 7 according to the following scheme:

$$\boxed{\begin{array}{ccc} N_3(P) & N_2(P) & N_1(P) \\ N_4(P) & P & N_0(P) \\ N_5(P) & N_6(P) & N_7(P) \end{array}}$$

Each N_i, $i = 0, \ldots, 7$, is a function from $\mathbb{Z}^2$ to $\mathbb{Z}^2$ that maps a point P to one of its neighbors according to this scheme.

First we restate some well-known definitions of measures of shape similarity for point sets. We define a **dilation** of a set X with radius r as $Dil^r(X) = \bigcup\{B(x, r) : x \in X\}$, where $B(x, r)$ denotes a closed ball of radius r centered at x in one of the above distances.

Hausdorff distance d_H of two planar sets A and B is given by

$$d_H(A, B) = \inf\{r \geq 0 : A \subseteq Dil^r(B) \text{ and } B \subseteq Dil^r(A)\}.$$

Since we are interested in shape similarity of planar sets modulo translation, we recall the definition of translation invariant *Hausdorff metric*:

$$H(X, Y) = \inf\{d_H(X + t, Y) : t \in \mathbb{R}^2\}.$$

In the following we introduce new concepts of *quadrant balls* and *directed dilation*.

Let $B_i(0, r)$ be the intersection of the closed ball of radius r in any of the three metrics with the closed $i-$th quadrant for $i = 1, 2, 3, 4$. Let $B_i(x, r) = B_i(0, r) + x$, where $x \in \mathbb{R}^2$. We will call $B_i(x, r)$ an $i-$th **quadrant ball**. The unit quadrant balls for the Euclidean distance are illustrated in Figure 1(a) and in L_∞ distance in Figure 2(a). We define a **directed dilation** of a set X with an $i-$th quadrant ball as $Dil_i^r(X) = \bigcup\{B_i(x, r) : x \in X\}$, e.g., see Figures 1 and 2.

Now we are going to introduce our novel definitions of distance measures based on directed dilation for subsets of the plane for $i, j = 1, 2, 3, 4$:

$h_i(X, Y) = \inf\{r \geq 0 : Y \subseteq Dil_i^r(X)\}$,

$h_{ij}(X, Y) = \max\{h_i(X, Y), h_j(Y, X)\}$, where $|i - j| = 2$, i.e., $(i, j) = (1, 3), (3, 1), (2, 4), (4, 2)$,

$H_{ij}(X, Y) = \inf\{h_{ij}(X + t, Y) : t \in \mathbb{R}^2\}$,

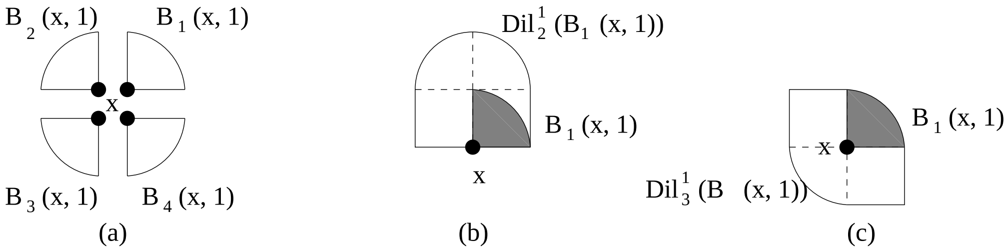

Figure 1: Unit quadrant balls in (a) and directed dilations in (b) and (c) are shown for the Euclidean distance.

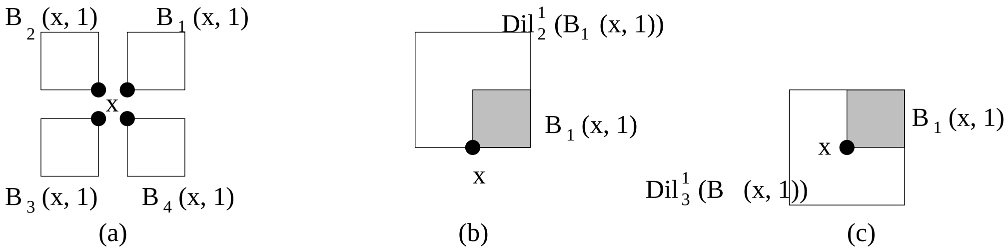

Figure 2: Unit quadrant balls in (a) and directed dilations in (b) and (c) are shown for the L_∞ distance.

$H_Q(X,Y) = \min\{H_{13}(X,Y), H_{31}(X,Y), H_{42}(X,Y), H_{24}(X,Y)\}$.

H_Q will be called (bidirectional) **quadrant Hausdorff distance**, shortly QH distance. In this paper, we use H_Q based on quadrant balls with respect to L_∞ metric unless explicitly stated otherwise.

Clearly, $H_Q(X,Y)$ is symmetric, since $H_{ij}(Y,X) = H_{ji}(X,Y)$ for $(i,j) = (1,3),(3,1),(2,4),(4,2)$. Another simple consequence of the definition is the fact that

$$H_Q(X,Y) = 0 \ \text{ iff } \ \exists v \in \mathbb{R}^2 \ X = Y + v,$$

since $H_{ij}(X,Y) = 0$ iff $\exists v \in \mathbb{R}^2 \ Y + v \subseteq X$ and $X \subseteq Y + v$ for $(i,j) = (1,3),(3,1),(2,4),(4,2)$.

3 Digitization and Hausdorff Distance

In this section we prove that two digital sets differ by at most quadrant Hausdorff distance one iff there exists a continuous set that digitizes to both of them. We recall that we base the quadrant Hausdorff distance H_Q on L_∞ metric.

Let $\mathcal{Q}$ be a cover of the plane with closed squares with the unit side length such that if two squares intersect, then their intersection is either their common side or a corner point. Such a cover is called a **square grid** with diameter r. A **digital image** can be described a set of points that are located at the centers of the squares of a grid $\mathcal{Q}$ and that are assigned some value in a gray level or color scale. We identify a digital image with the set $\mathbb{Z}^2$. We also interpret a point p in $\mathbb{Z}^2$ as a closed (black) square of cover $\mathcal{Q}$ centered at p.

By a **digitization process** we understand a function mapping a planar set X to a digital image. A square $p \in \mathcal{Q}$ is black (belongs to a digital object) iff $p \cap X \neq \emptyset$, and white otherwise. We will call such a digital image an **(intersection) digitization** of set X, and denote it with $Dig(X)$, namely $Dig(X) = \bigcup\{p \in \mathcal{Q} : p \cap X \neq \emptyset\}$. The detailed discussion and motivations for this mathematical model of digitization process can be found in Gross and Latecki [1] and Latecki et al. [4].

The goal of this section is to prove our main theorem:

Theorem 1 *Let A and B be two digital sets, i.e., finite subsets of $\mathbb{Z}^2$, $H_Q(A, B) \leq 1$ iff there exist a planar set X and a vector $v \in \mathbb{R}^2$ such that $Dig(X) = A$ and $Dig(X + v) = B$.*

Proof: The theorem follows from Propositions 1 and 2 below. ∎

Theorem 1 does not hold for Hausdorff distance H, since there exist digital sets A and B such that $H(A, B) \leq 1$ and no continuous set digitizes to both of them. Examples of two elementary sets A and B are given in Figure 3. Since B is a single grid square, the set X that digitizes to B must be contained in the interior of the grid square. However, no set contained in the interior of the grid square can intersect all the nine squares in set A. By union of the elementary sets A and B, digital sets X and Y of arbitrary shape can be constructed such that $H(X, Y) \leq 1$.

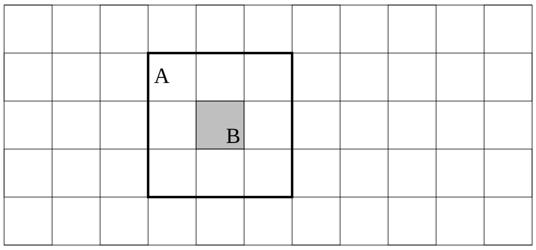

Figure 3:

Proposition 1 *Let A and B be two digital sets. If $H_Q(A, B) \leq 1$, then there exist a planar set X and a vector $v \in \mathbb{R}^2$ such that $Dig(X) = B$ and $Dig(X + v) = A$.*

Proof: Without loss of generality, we can assume that $h_{24}(B, A) \leq 1$.

The proof is illustrated on the example sets in Figure 4. Set A is enclosed by the bold boundary curve, set B is composed of gray squares, and the continuous set X is the union of black bullets.

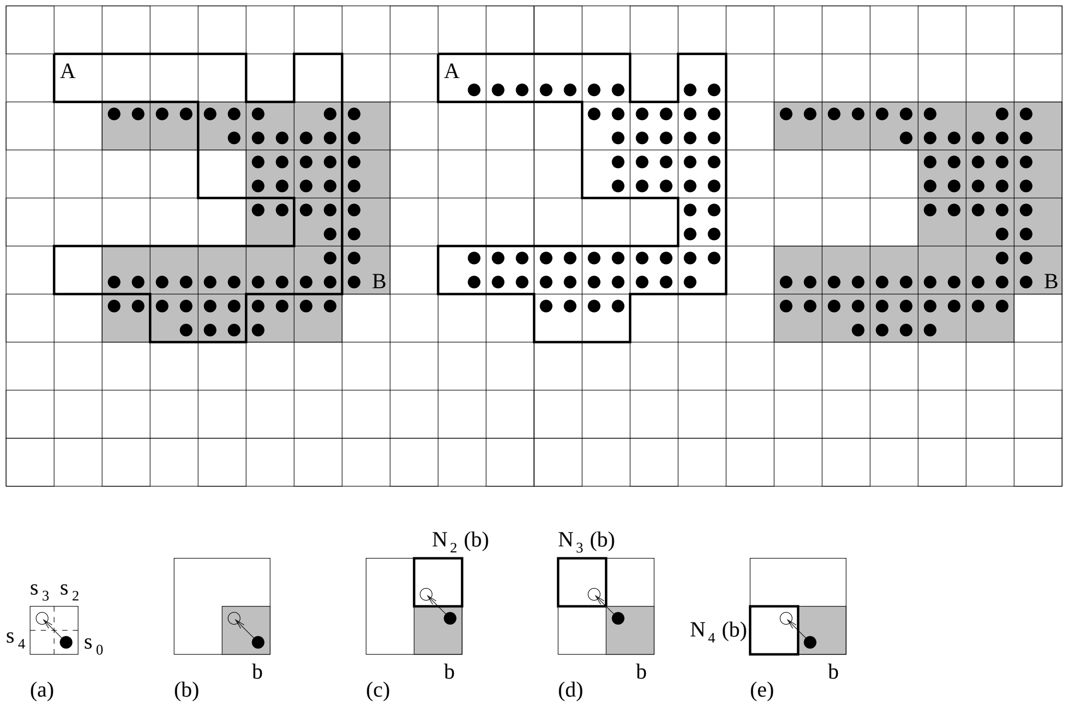

Figure 4: For the set X that is the union of black bullets holds: $Dig(X) = B$ and $Dig(X+v) = A$, where $v =< -\frac{1}{2}, \frac{1}{2} >$.

As vector v we take $v =< -\frac{1}{2}, \frac{1}{2} >$. We describe first the process of constructing the set X such that $Dig(X) = B$ and $Dig(X+v) = A$.

We divide each grid square q to four equal squares $s_0(q), s_2(q), s_3(q), s_4(q)$ called **small squares**, see Figure 4(a). A **bullet** is a closed ball with the center at the center of one of the small squares that is completely contained in this square.

Set X is the union of bullets obtained in the following way. (see Figure 4(b)-(e)). For a given square $b \in B$:

1. a bullet is contained in $s_0(b)$ iff $b \in A$ and

2. a bullet is contained at $s_i(b)$ iff $N_i(b) \in A$ for $i = 2, 3, 4$.

Since for every $b \in B$, at least one square $b, N_2(b), N_3(b), N_4(b)$ belongs to A, due to the assumption $h_{24}(B, A) \leq 1$, at least one bullet is contained in b. Hence $Dig(X) = B$.

The fact that $Dig(X + v) = A$ follows from the following observations (see Figure 4(b)-(e)):

1. a bullet α is contained in $s_0(b)$ iff $\alpha + v$ is contained in b and

2. a bullet α is contained in $s_i(b)$ iff $\alpha + v$ is contained in $N_i(b)$ for $i = 2, 3, 4$

Thus, we have shown that $Dig(X) = B$ and $Dig(X + v) = A$. ■

As proved in [4] (see also [1]), if the resolution of a digitization process is sufficient, then the resulting segmented digital image and the underlying continuous object are topologically equivalent. Moreover, the obtained digital image is well-composed, where a binary digital image is **well-composed** if it does not contain the checkerboard pattern shown in Figure 5 nor its 90^o rotation [4]. The mathematical model of the digitization and segmentation process used in [4] includes the intersection digitization used in this paper.

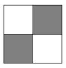

Figure 5: This pattern and its 90^o rotation do not occur in a well-composed digital image.

The set X defined in the proof of Proposition 1 is not connected. If both digital sets A and B are well-composed, then there exists a connected set X' such that $Dig(X') = B$ and $Dig(X' + v) = A$. We obtain the set X' from the set X in the following way:

Set X' is the union of horizontal and vertical line segments of length smaller than one whose endpoints are contained in X.

If on of the digital sets A and B is not well-composed, then there does not exist a connected continuous set X such that $Dig(X) = B$ and $Dig(X + v) = A$, as it is illustrated in Figure 6.

Proposition 2 *For every planar set X and for every vector $v \in \mathbb{R}^2$ we have*

$$H_Q(Dig(X), Dig(X + v)) \leq 1.$$

Proof: First observe that if $t \in \mathbb{Z}^2$, then $Dig(X) + t = Dig(X + t)$. This is illustrated in Figure 7, where $t \in \mathbb{Z}^2$ and $v \notin \mathbb{Z}^2$.

Let $v = (v_1, v_2) \in \mathbb{R}^2$, $t = (\lfloor v_1 \rfloor, \lfloor v_2 \rfloor)$, and let $u = (v_1 - \lfloor v_1 \rfloor, v_2 - \lfloor v_2 \rfloor)$ (see Figure 8(a)). Then both coordinates of u are less or equal to one.

Since H_Q is invariant with respect to translation and $Dig(X) + t = Dig(X + t)$, we obtain $H_Q(Dig(X), Dig(X + v)) = H_Q(Dig(X), Dig(X + (t + u))) = H_Q(Dig(X), Dig(X + u) + t) = H_Q(Dig(X), Dig(X + u))$.

Thus, it is sufficient to show that $H_Q(Dig(X), Dig(X + u)) \leq 1$.

We can assume without loss of generality that u is contained in the first quadrant. If $x \in X$ and s is a grid square containing x, then $x + u$ is contained in $B_1(s, 1)$, since both coordinates of u are less or equal to 1 (see Figure 8(b)). Thus,

$$Dig(\{x + u\}) \subseteq Dil_1^1(Dig(\{x\}) = B_1(s, 1).$$

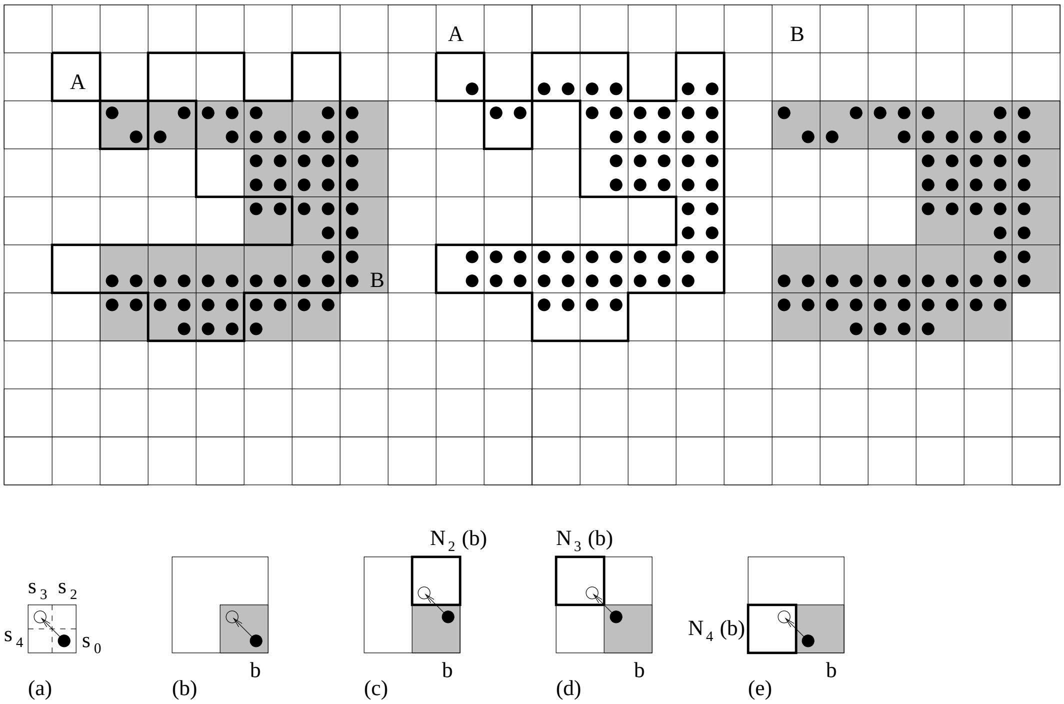

Figure 6: Since set A is not well-composed, there does not exist a connected continuous set X such that $Dig(X) = B$ and $Dig(X + v) = A$.

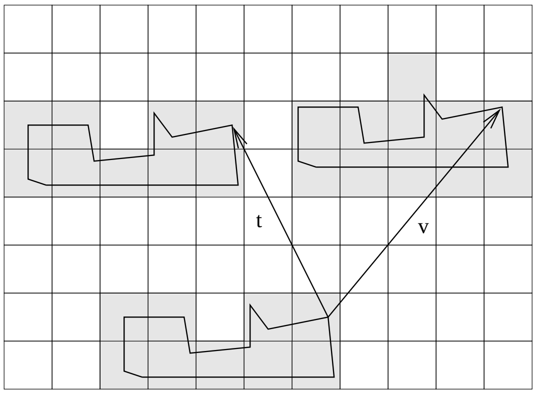

Figure 7: $Dig(X) + t = Dig(X + t)$, since $t \in \mathbb{Z}^2$.

Since $x = (x + u) - u$ and $-u$ is contained in the third quadrant, we obtain

$$Dig(\{x\}) \subseteq Dil_3^1(Dig(\{x + u\}).$$

Since these inclusions hold for every $x \in X$, we obtain

$$Dig(X + u) \subseteq Dil_1^1(Dig(X) \quad \text{and} \quad Dig(X) \subseteq Dil_3^1(Dig(X + u),$$

and consequently, $H_Q(Dig(X), Dig(X + u)) \leq 1$. ∎

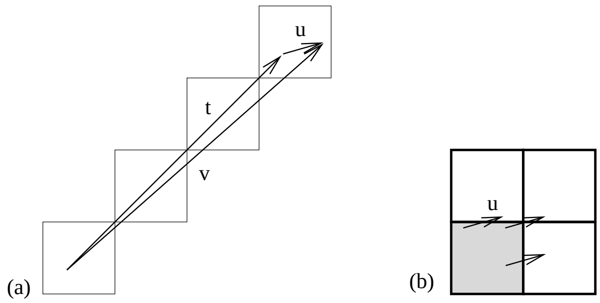

Figure 8:

4 H_Q is a Metric for the L_∞ Distance

First we show that $H_Q(X,Y)$ is not a metric if it is based on the Euclidean metric, since it does not satisfy triangular inequality. For the sets $\{x\}, B_1(x,1), Dil_2^1(B_1(x,1))$ shown in Figure 1(b) we have

$$H_Q(\{x\}, B_1(x,1)) = H_{13}(\{x\}, B_1(x,1)) = 1$$

and

$$H_Q(B_1(x,1), Dil_2^1(B_1(x,1))) = H_{24}(B_1(x,1), Dil_2^1(B_1(x,1))) = 1.$$

Therefore,

$$H_Q(\{x\}, B_1(x,1)) + H_Q(B_1(x,1), Dil_2^1(B_1(x,1))) = 2 < H_Q(\{x\}, Dil_2^1(B_1(x,1))).$$

The same holds for the sets $\{x\}, B_1(x,1), Dil_3^1(B_1(x,1))$ in Figure 1(c).

The main result of this sections is the following:

Theorem 2 *H_Q is a metric if it is based on the L_∞ distance.*

This theorem follows from Proposition 3 below, since as we noticed in Section 2, H_Q is symmetric and $H_Q(X,Y) = 0$ iff $\exists v \in \mathbb{R}^2\ X = Y + v$.

Proposition 3 *H_Q satisfies triangular inequality if it is based on the L_∞ distance:*

$$H_Q(A,B) + H_Q(B,C) \geq H_Q(A,C).$$

Proof: Due to the definition of H_Q, we have $H_Q(A,B) = H_{ij}(A,B)$ and $H_Q(B,C) = H_{kl}(B,C)$, where $(i,j),(k,l) \in \{(1,3),(3,1),(2,4),(4,2)\}$.
If $(i,j) = (k,l)$, then

$$H_{ij}(A,B) + H_{ij}(B,C) \geq H_{ij}(A,C) \geq H_Q(A,C),$$

by Proposition 6, below. Thus, it remains to prove the inequality for $(i,j) \neq (k,l)$. First we show the inequality for
$(i,j) = (1,3)$ and $(k,l) = (3,1), (2,4), (4,2)$.
Then we show that the other cases reduce to one of the three cases. To focus our attention, let us assume that $H_Q(A,B) = H_{13}(A,B) = r_{13}$. We need to show the statement for

1. $H_Q(B,C) = H_{31}(B,C) = r_{31}$,
2. $H_Q(B,C) = H_{24}(B,C) = r_{24}$,
3. $H_Q(B,C) = H_{42}(B,C) = r_{42}$.

Since the proof for these three cases follow the same schema, we will state it only for the second case.
Let $H_Q(A,B) = H_{13}(A,B) = r_{13}$ and let $H_Q(B,C) = H_{24}(B,C) = r_{24}$. We will show that $r_{13} + r_{24} \geq H_{24}(A,C) \geq H_Q(A,C)$.
$H_{13}(A,B) = r_{13}$ implies

$$\exists v \in \mathbb{R}^2 \; [B \subseteq Dil_1^{r_{13}}(A+v) \;\text{ and }\; A+v \subseteq Dil_3^{r_{13}}(B)] \tag{1}$$

and $H_{24}(B,C) = r_{24}$ implies

$$\exists u \in \mathbb{R}^2 \; [C+u \subseteq Dil_2^{r_{24}}(B) \;\text{ and }\; B \subseteq Dil_4^{r_{24}}(C+u)] \tag{2}$$

If we dilate the left inclusion in (1) by $Dil_2^{r_{24}}$, we obtain

$$Dil_2^{r_{24}}(B) \subseteq Dil_2^{r_{24}}(Dil_1^{r_{13}}(A+v)),$$

which by the left inclusion in (2) implies

$$C+u \subseteq Dil_2^{r_{24}}(Dil_1^{r_{13}}(A+v)).$$

By Lemma 1.2.a below,

$$Dil_2^{r_{24}}(Dil_1^{r_{13}}(A+v)) = Dil_2^{r_{13}+r_{24}}(A+v+(r_{13},0)).$$

Thus,

$$C+u \subseteq Dil_2^{r_{13}+r_{24}}(A+v+(r_{13},0)). \tag{3}$$

Similarly, the right inclusion in (2) and the right inclusion in (1) imply

$$A+v \subseteq Dil_3^{r_{13}}(Dil_4^{r_{24}}(C+u)),$$

and by Lemma 1.2.b below,

$$A + v \subseteq Dil_4^{r_{13}+r_{24}}(C + u - (r_{13}, 0)),$$

which implies

$$A + v + (r_{13}, 0) \subseteq Dil_4^{r_{13}+r_{24}}(C + u) \tag{4}$$

By formulas (3) and (4), we obtain that $r_{13} + r_{24} \geq H_{24}(A, C)$.

If $H_Q(A, B) = H_{13}(A, B) = r_{13}$ and $H_Q(B, C) = H_{31}(B, C) = r_{31}$, then it can be shown following the above scheme and using Lemma 1.1 that $r_{13} + r_{31} \geq H_{31}(A, C) \geq H_Q(A, C)$.

If $H_Q(A, B) = H_{13}(A, B) = r_{13}$ and $H_Q(B, C) = H_{42}(B, C) = r_{42}$, then it can be shown following the above scheme and using Lemma 1.3 that $r_{13} + r_{42} \geq H_{42}(A, C) \geq H_Q(A, C)$.

Thus, we have shown the triangular inequality for the indices $(i, j) + (k, l)$ of $H_{ij}(A, B)$ and $H_{kl}(B, C)$ being equal to

$(1, 3) + (3, 1), (1, 3) + (2, 4), (1, 3) + (4, 2)$.

Following the same scheme, we can prove the triangular inequality for the indices

$(3, 1) + (2, 4), (3, 1) + (4, 2), (2, 4) + (4, 2)$.

The remaining cases listed below coincide with the above ones, due to the symmetry of the addition, i.e., $(3, 1) + (1, 3)$ coincides with $(1, 3) + (3, 1)$:

$(3, 1) + (1, 3)$

$(2, 4) + (1, 3), (2, 4) + (3, 1)$

$(4, 2) + (1, 3), (4, 2) + (3, 1), (4, 2) + (2, 4)$. ■

Lemma 1 *The following equations all hold*

(1.a) $Dil_3^s(Dil_1^r(X)) = Dil_3^{r+s}(X + (r, r)) = Dil_1^{r+s}(X - (s, s))$ *and*

(1.b) $Dil_3^r(Dil_1^s(Y)) = Dil_3^{r+s}(Y + (s, s)) = Dil_1^{r+s}(Y - (r, r))$ *(e.g., Figures 9)*

(2.a) $Dil_2^s(Dil_1^r(X)) = Dil_2^{r+s}(X + (r, 0)) = Dil_1^{r+s}(X - (s, 0))$ *and*

(2.b) $Dil_3^r(Dil_4^s(Y)) = Dil_3^{r+s}(Y + (s, 0)) = Dil_4^{r+s}(Y - (r, 0))$ *(e.g., Figure 10)*

(3.a) $Dil_4^s(Dil_1^r(X)) = Dil_4^{r+s}(X + (0, r)) = Dil_4^{r+s}(X - (0, s))$ *and*

(3.b) $Dil_3^r(Dil_2^s(Y)) = Dil_3^{r+s}(Y + (0, s)) = Dil_2^{r+s}(Y - (0, r))$ *(e.g., Figures 11)*

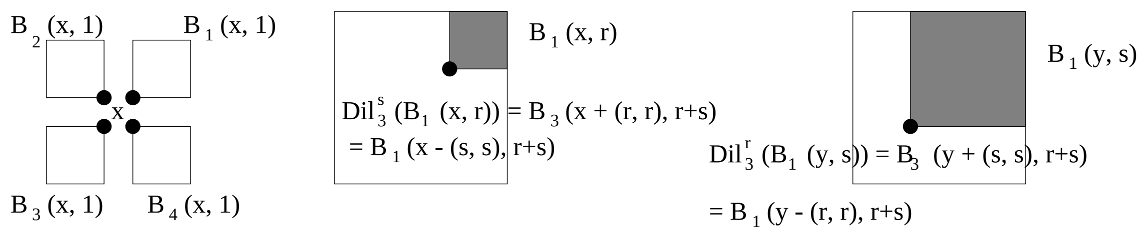

Figure 9:

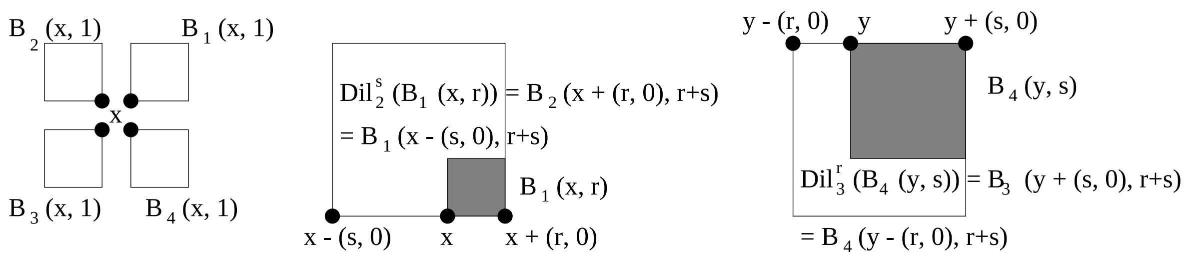

Figure 10:

Proof: We prove only equation (2.a) of this lemma. The proof of the other equations is similar. It is sufficient to observe that for every $x \in X$ (see Figure 10(middle)):

$Dil_2^s(Dil_1^r(\{x\})) = Dil_2^s(B_1(x,r)) = B_2(x + (r,0), r + s) = Dil_2^{r+s}(\{x\} + (r,0))$

We also have $B_2(x + (r,0), r + s) = B_1(x - (s,0), r + s) = Dil_1^{r+s}(\{x\} - (s,0))$

The proof of (2.b) is illustrated also in Figure 10(right). The proofs of equations (1.a), (1.b), (3.a), and (3.b) are illustrated also in Figures 9 and 11. ■

Below we show that h_{ij} satisfies triangle inequality by Proposition 5, and that H_{ij} satisfies triangle inequality by Proposition 6.

Proposition 4 *If* $h_i(A,B) < \infty$ *and* $h_i(B,C) < \infty$ *and* $i = 1,2,3,4$, *then*

$$h_i(A,B) + h_i(B,C) \geq h_i(A,C),$$

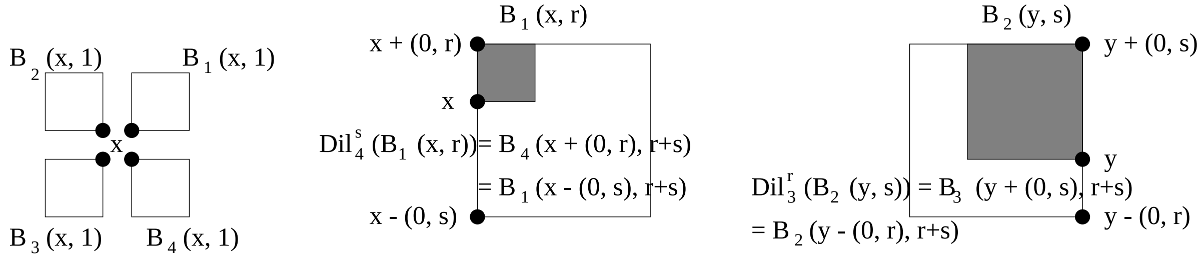

Figure 11:

and in particular, $h_i(A,C) < \infty$.

Proof: To focus our attention, we assume that $i = 4$. Let $h_4(A,B) < \infty$ and $h_4(B,C) < \infty$. We will show that

$$h_4(A,B) + h_4(B,C) \geq h_4(A,C).$$

An example is given in Figure 12.

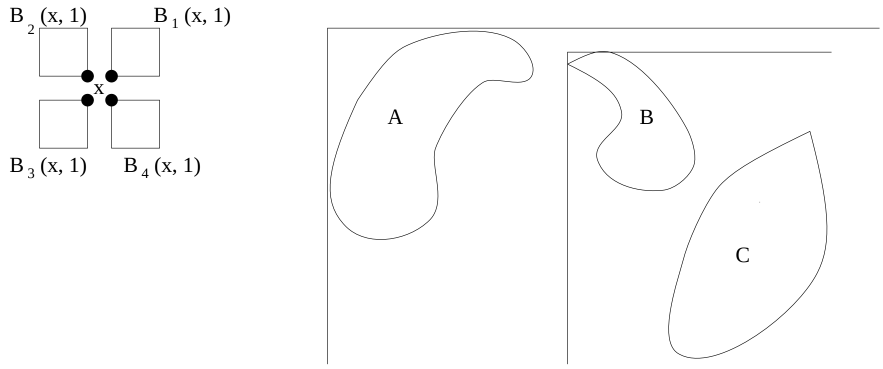

Figure 12:

Let r_1 and r_2 be such that $B \subseteq Par_4(A, r_1)$ and $C \subseteq Par_4(B, r_2)$,
which means that $B \subseteq \bigcup_{x\in A} B_4(x, r_1)$ and $C \subseteq \bigcup_{x\in b} B_4(x, r_2)$.
The inclusion $B \subseteq \bigcup_{x\in A} B_4(x, r_1)$ implies, for every $x \in B$, $B_4(x, r_2) \subseteq \bigcup_{x\in A} B_4(x, r_1 + r_2)$. Thus,

$$C \subseteq \bigcup_{x\in b} B_4(x, r_2) \subseteq \bigcup_{x\in A} B_4(x, r_1 + r_2).$$

Therefore, if $r_1 \in \{r \geq 0 : B \subseteq Par_4(A, r)\}$ and $r_2 \in \{r \geq 0 : C \subseteq Par_4(B, r)\}$,
then $r_1 + r_2 \in \{r \geq 0 : C \subseteq Par_4(A, r)\}$. Hence,

$$\inf\{r \geq 0 : A \subseteq Par_4(A, r)\} + \inf\{r \geq 0 : C \subseteq Par_4(B, r)\} \geq \inf\{r \geq 0 : C \subseteq Par_4(A, r)\}.$$

■

Proposition 5 *For every triple of planar sets* A, B, C *and* $(i, j) \in \{(1,3),(3,1),(2,4),(4,2)\}$ *we have*

$$h_{ij}(A,B) + h_{ij}(B,C) \geq h_{ij}(A,C)$$

if $h_{ij}(A,B) < \infty$ *and* $h_{ij}(B,C) < \infty$.

Proof: To focus our attention, we assume that $(i, j) = (4, 2)$, i.e., we will show that

$$h_{42}(A, B) + h_{42}(B, C) \geq h_{42}(A, C).$$

By Preposition 4, we have

$$\begin{aligned} h_4(A, B) + h_4(B, C) &\geq h_4(A, C) \\ h_2(B, A) + h_2(C, B) &\geq h_2(C, A). \end{aligned}$$

Since $\max\{h_4(A, C), h_2(C, A)\}$ is smaller or equal to one of the two left sides, we obtain

$$\max\{h_4(A, B), h_2(B, A)\} + \max\{h_4(B, C), h_2(C, B)\} \geq \max\{h_4(A, C), h_2(C, A)\}.$$

■

Proposition 6 *For every triple of planar sets A, B, C and for $(i, j) \in \{(1, 3), (3, 1), (2, 4), (4, 2)\}$, we have*

$$H_{ij}(A, B) + H_{ij}(B, C) \geq H_{ij}(A, C).$$

Proof: To focus our attention, we assume that $(i, j) = (4, 2)$, i.e., we will show that

$$H_{42}(A, B) + H_{42}(B, C) \geq H_{42}(A, C).$$

Let $\epsilon > 0$. There exist $v, u \in \mathbb{R}^2$ such that
$H_{42}(A, B) + \epsilon/2 > h_{42}(A + v, B)$ and $H_{42}(B, C) + \epsilon/2 > h_{42}(B, C + u)$.
Then $H_{42}(A, B) + H_{42}(B, C) > h_{42}(A + v, B) + h_{42}(B, C + u) - \epsilon$. By Proposition 5, we have $h_{42}(A + v, B) + h_{42}(B, C + u) \geq h_{42}(A + v, C + u)$. Thus,

$$H_{42}(A, B) + H_{42}(B, C) > h_{42}(A + v, C + u) - \epsilon \geq H_{42}(A, C) - \epsilon$$

Since this is the case for every $\epsilon > 0$, we obtain

$$H_{42}(A, B) + H_{42}(B, C) \geq H_{42}(A, C).$$

■

5 Experimental Results

In this section we present experimental results that confirm the implications of Theorem 1. The "$\Leftarrow$" implication says that any two digital images of the same planar object can differ by at most quadrant Hausdorff distance one.

We carried a large number of experiments with a scanner as a digitization device. We obtained different digital images by translating a given object and scanning it. For example, the four digital images in Figure 13 are scanner digitizations of the same underlying ellipse printed on the paper four times. Image (b) happened to retain the perfect ellipse digitization, i.e., the original model shape before digitization was exactly as in (b). Images (a), (c), and (d) have residual pixels, i.e., minimal difference modulo translation instance minus the model shape and the model shape minus instance are indicated by residual pixels of two different gray-values. Figure 13 demonstrates that after digitization shapes do not differ from the underlying model by more than one in the quadrant Hausdorff measure. Thus, Figure 13 illustrates that the proposed quadrant Hausdorff measure applies as a similarity measure to real scanner images.

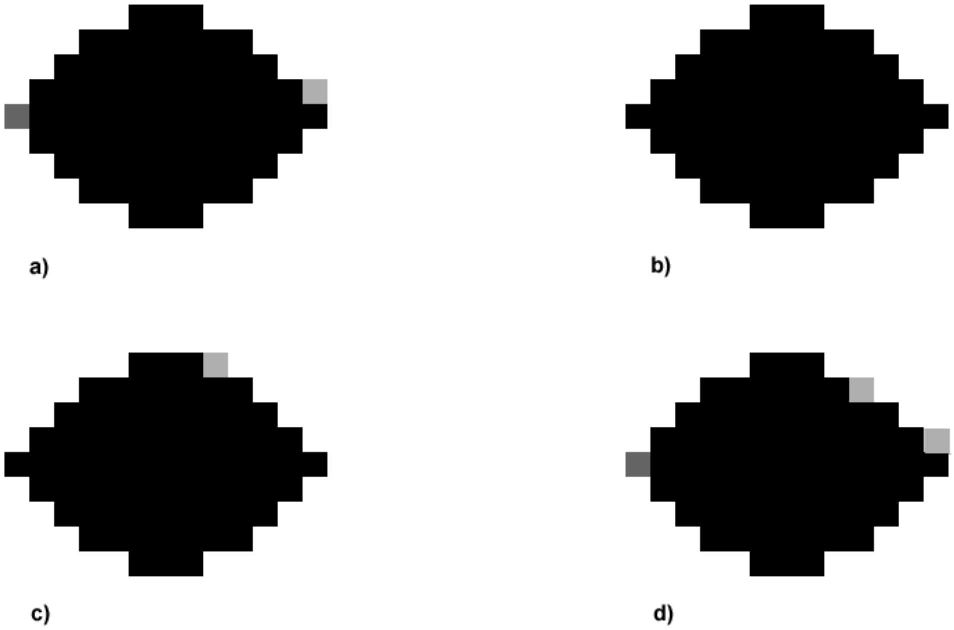

Figure 13:

Acknowledgments

We would like to thank Ruben Lusinyants and Navdeep Sing Tinna for the implementation of the experimental results.

References

[1] A. Gross and L. Latecki. Digitizations Preserving Topological and Differential Geometric Properties. *Computer Vision and Image Understanding* 62, 370–381, 1995.

[2] D. Huttenlocher and G. Klanderman and W. Rucklidge. Comparing Images Using the Hausdorff Distance. *IEEE Trans. PAMI* 15, 850–863, 1993.

[3] L. Latecki, U. Eckhardt, and A. Rosenfeld. Well-Composed Sets. *Computer Vision and Image Understanding* 61, 70–83, 1995.

[4] L. J. Latecki, C. Conrad, and A. Gross, Preserving Topology by a Digitization Process. *Journal of Mathematical Imaging and Vision* 8, 131–159, 1998.

[5] W. Rucklidge. *Efficient Visual Recognition Using the Hausdorff Distance.* Number 1173 in Lecture Notes in Computer Science. Springer-Verlag, 1996.